

# Earthquake Resistant Performance of Reinforced Concrete Frame Strengthened by Multi-Story Steel Brace

KITAYAMA Kazuhiro <sup>\*1</sup>, KISHIDA Shinji <sup>\*2</sup> and SATO Teruyoshi <sup>\*3</sup>

## ABSTRACT

Earthquake resistant performance in plane R/C frames strengthened by multi-story steel brace was investigated through the tests under cyclic load reversals focusing on the base uplift rotation of the brace and the entire flexural failure at the bottom of the brace caused by tensile yielding of all longitudinal bars in a R/C edge column beside the brace. Two plane frame specimens with two-story and three-bay were tested placing multi-story steel brace at the central bay. Lateral resistance in base uplift rotation of a multi-story brace decreased gradually after flexural yielding at the end of boundary beams and the bottom of first story bare columns. Lateral strength measured in the specimen agreed well with that computed by taking account of restraining effect of both boundary and foundation beams on uplift rotation. For another specimen failed in entire flexure at the bottom of the brace, controlled by tensile yielding of all longitudinal bars in a R/C edge column beside a brace, lateral resistance diminished abruptly by concrete compressive crushing and fracture of column longitudinal bars at the bottom of both edge columns. Ultimate limit deformations in two specimens were underestimated by the computation considering deformation ability of neighboring beams and isolated multi-story steel brace. The amount of energy dissipation for entire flexural failure at the bottom of a brace was by 50 percent greater than that for base rotation failure. Earthquake resistant performance of strengthened R/C frames which is controlled by the entire flexural failure at the bottom of a multi-story steel brace is superior to that in the failure due to the brace uplift rotation within the range of the drift angle of 2 %.

## 1. INTRODUCTION

For seismic retrofit of existing reinforced concrete (R/C) buildings, steel braces enclosed by perimeter steel rims are often installed into moment resisting open frames. It is most desirable that the one of diagonal chords of steel braces yields in tension and the other buckles in compression under earthquake excitations. Unfortunately the base of a multi-story steel brace may be uplifted and rotate in some cases prior to the yielding or buckling of steel chords depending primarily on the aspect ratio of the span to the height. In other cases, the strength of a multi-story steel brace is attributed to entire flexural resistance in I-

---

*\*1 Associate Professor, Graduate School of Engineering, Tokyo Metropolitan University, Dr. Eng.*

*Email : kitak@ecomp.metro-u.ac.jp*

*\*2 Research Associate, Graduate School of Engineering, Tokyo Metropolitan University, Dr. Eng.*

*Email : skishida@ecomp.metro-u.ac.jp*

*\*3 Graduate student, Tokyo Metropolitan University*

*Email : te-ru@dc5.so-net.ne.jp*

shaped section at the bottom of a unit bay consisting of a steel brace and R/C edge columns, which is induced by tensile yielding of all longitudinal bars in a R/C edge column (called as the failure of Type 3) before the full capacity of a steel brace can be developed.

In the paper, earthquake resistant performance of R/C frames strengthened by a multi-story steel brace, which were designed to develop uplift rotation of a base foundation beneath a multi-story steel brace or the failure of Type 3, was studied by static load reversal tests.

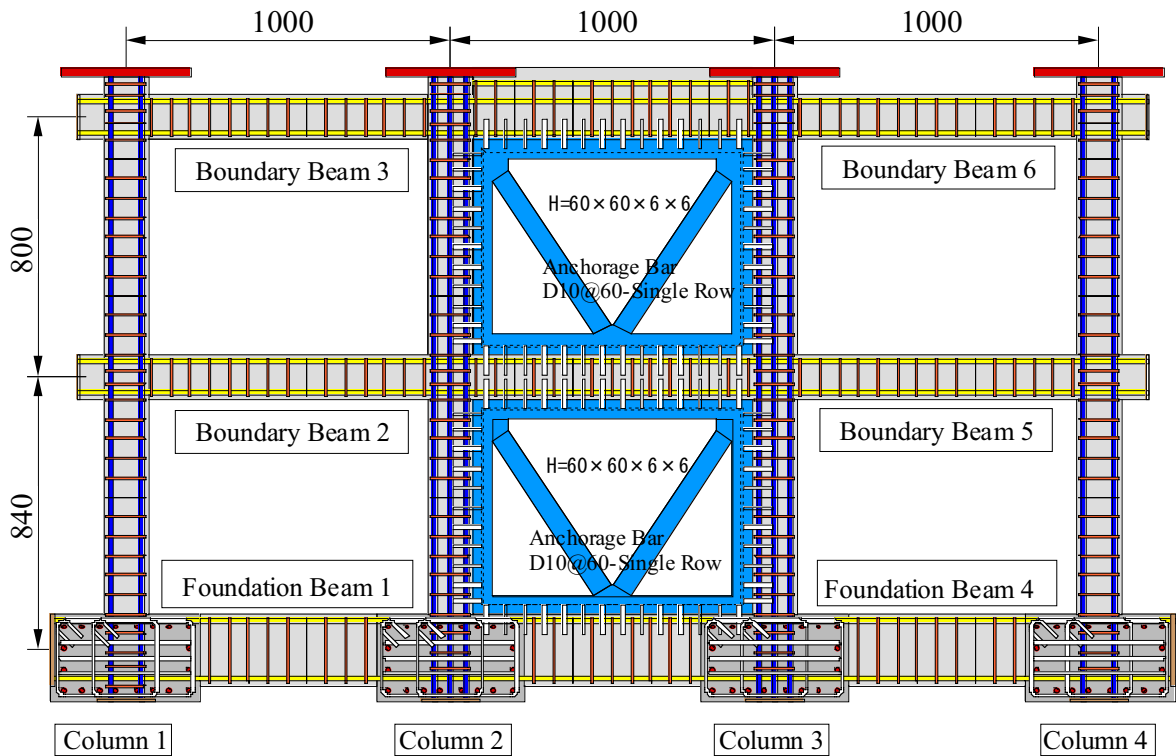
## 2. OUTLINE OF TEST

### 2.1 SPECIMENS

Reinforcement details and section dimensions are shown in **Fig. 1**. Two plane frame specimens with a quarter scale to actual buildings were tested which had three bays with each 1000 mm span length and two stories with the height of 800 mm, placing a multi-story steel brace at the central bay. Section dimensions of R/C beams and columns and steel brace were common for two specimens except for the amount of longitudinal reinforcement of R/C edge columns beside a steel brace (denoted as Column 2 and 3 in **Fig. 1**).

The failure type of R/C central bay containing a multi-story steel brace was chosen as a test parameter. Specimen No.1 was designed to develop the rotation of base foundation due to the uplift of a multi-story steel brace. On the other hand, Specimen No.2 was designed to result in entire flexural failure at the bottom of a multi-story steel brace which is caused by both yielding of all longitudinal bars in a R/C tensile edge column and pull-out of anchorage bars connecting between horizontal steel rim of a brace and R/C foundation beam. The amount of longitudinal bars in edge columns beside the brace was reduced in Specimen No.2 comparing with those in Specimen No.1 in order to cause the failure of Type 3. Boundary beams and isolated columns were designed according to the weak-beam strong-column concept.

Cross section of a steel brace was a H-shape with 60 mm width and 60 mm depth, which was built by welding flat plates with 6 mm thickness. Details of connection between R/C member and steel rim are illustrated by **Fig. 2**. Anchorage bars of D10 were welded in a row to perimeter steel rims with the center-to-center spacing of 60 mm. Although non-shrinkage mortar is injected between steel rims and R/C members to unify each other for actual practice, mortar injection was omitted in construction of specimens by casting concrete in the state that steel braces were placed at proper position with reinforcement



	Boundary Beam(2,3,5,6)	Foundation Beam(1,4)
Section		
	Pt=2.38% / pw=1.05%	Pt=1.42% / pw=1.05%

	Column 1 and 4 (common)	Column 2 and 3 (Specimen No.1)	Column 2 and 3 (Specimen No.2)
Section			
	Pt=1.29% / pw=0.67%	Pt=1.29% / pw=0.67%	Pt=0.73% / pw=0.67%

**Fig. 1 Reinforcement details and section dimensions**

**Table 1 Material properties of steel and concrete**

(a) Steel

	Bar size	Yield strength MPa	Young's modulus GPa	Yield strain %
Longitudinal bar in edge column	*D13	336.1	180	0.187
	**D10	367.8	185	0.199
Longitudinal bar in bare column	D13	429.1	179	0.239
Beam longitudinal bar	D13	345.6	184	0.188
Anchorage bar	D10	383.2	188	0.204
Shear reinforcing bar	R6	588.7	207	0.284
Steel brace	flat bar	435.3	208	0.209

(b) Concrete

Specimen	Compressive strength MPa	Strain at compressive strength %	Secant modulus GPa	Tensile strength MPa
No.1	28.9	0.195	30.5	1.97
No.2	30.3	0.216	28.0	2.43

\* : Specimen No.1 , \*\* : Specimen No.2

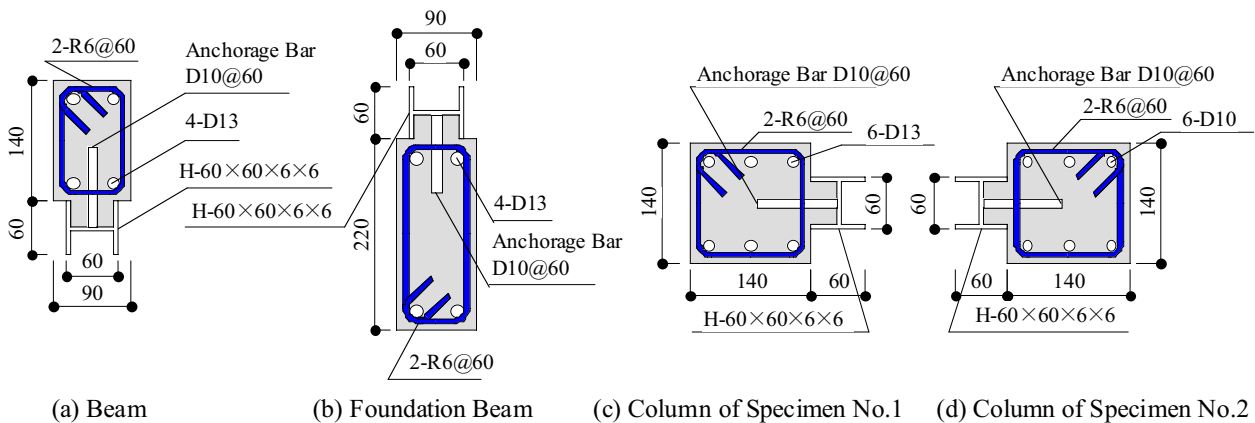


**Fig. 2 Details of connection between R/C members and steel rim**

cages of beams and columns. Concrete was cast in the horizontal position using metal casting form. Material properties of concrete and steel are listed in **Table 1**. Concrete compressive strength was 30 MPa approximately by cylinder tests.

## 2.2 LOADING METHOD AND INSTRUMENTATION

The loading system is shown in **Fig. 3**. Top lateral force was applied alone at the center of the specimen by two oil jacks. Each column axial load was kept constant, i.e., 40 kN to isolated columns and 80 kN to edge columns beside a steel brace respectively. Four footings of Specimen No.2 were fixed to R/C reaction floor by PC tendons. For Specimen No.1 designed to cause the uplift of a multi-story steel brace, on the other hand, two footings under the steel brace were not connected to the floor, but lateral reaction force was supported through round steel bar inserted between R/C footing subjected to axial compression and steel reaction plate settled on reaction floor. This testing method was accepted by referring to the study carried out by Kato [1].

Specimen was controlled by the drift angle for one cycle of 0.25 %, two cycles of 0.5 %, 1 % and 2 % respectively and one cycle of 4 %. The drift angle is defined as the horizontal

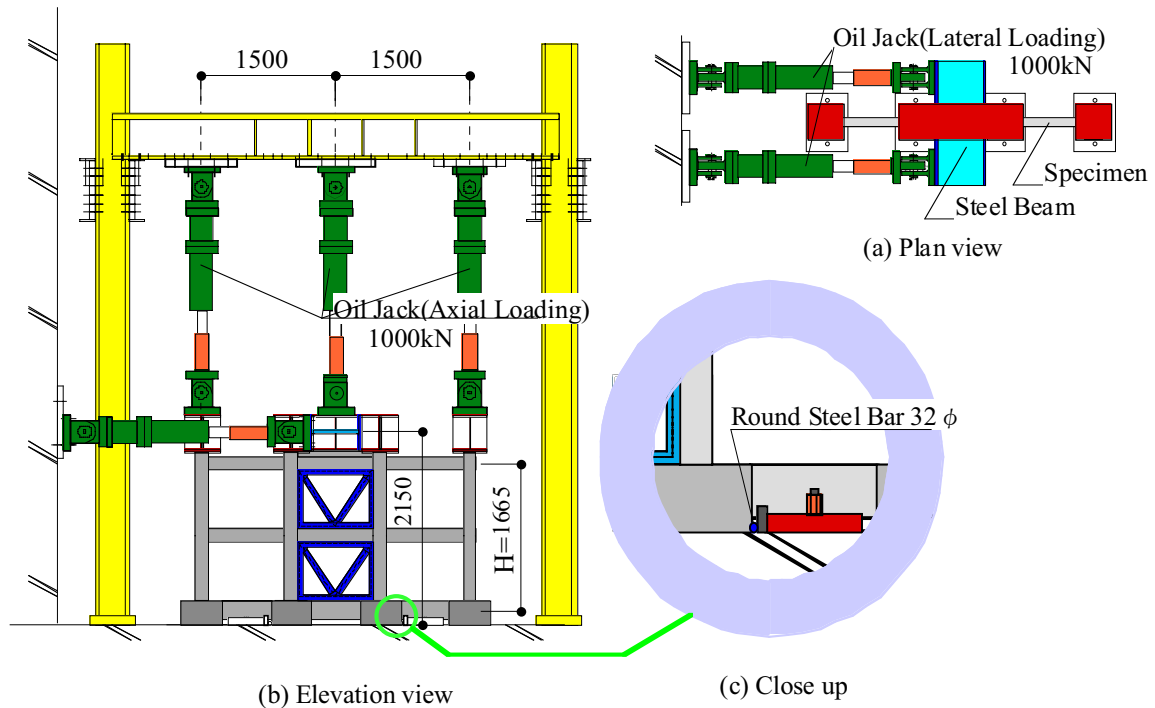


**Fig. 3 Loading apparatus**

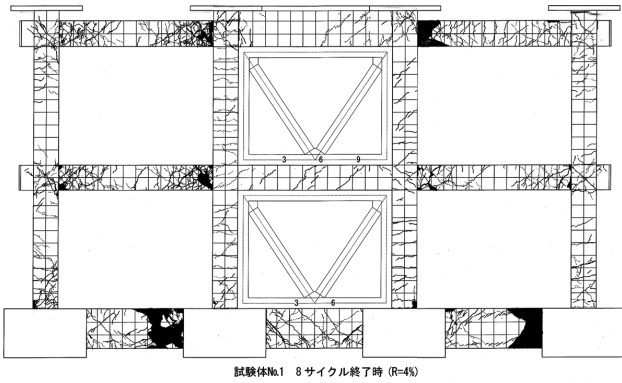
displacement at the center of a top floor beam divided by the height between the center of a foundation beam and a top floor beam, i.e., 1665 mm.

Lateral force and column axial load were measured by load-cells. Horizontal displacement at load applying point and at the center of top and second floor beams, local rotation in a plastic hinge region of beams and columns, and vertical displacement of footings due to uplift of a steel brace were measured by displacement transducers. Strains of beam and column longitudinal bars, vertical and diagonal steel chords of a brace and anchorage bars at the bottom of a first-story steel brace were measured by strain gauges.

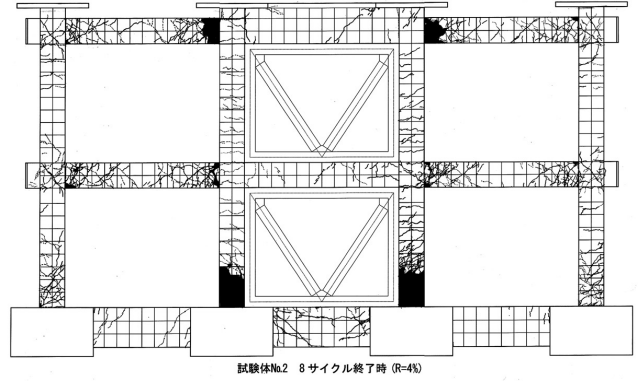
### 3. TEST RESULTS

#### 3.1 PROCESS TO FAILURE AND STORY SHEAR - DRIFT RELATIONS

Crack patterns at the end of test are shown in **Fig. 4** and **Photo. 1**. Story shear force - drift angle relations are shown in **Fig. 5** for cyclic load reversals and **Fig. 6** as an envelope curve in positive loading illustrating successive phenomena occurred in the specimen. Story shear force in this paper is defined as the horizontal force applied by oil jacks corrected for the P-Delta effect resulted from column axial load.

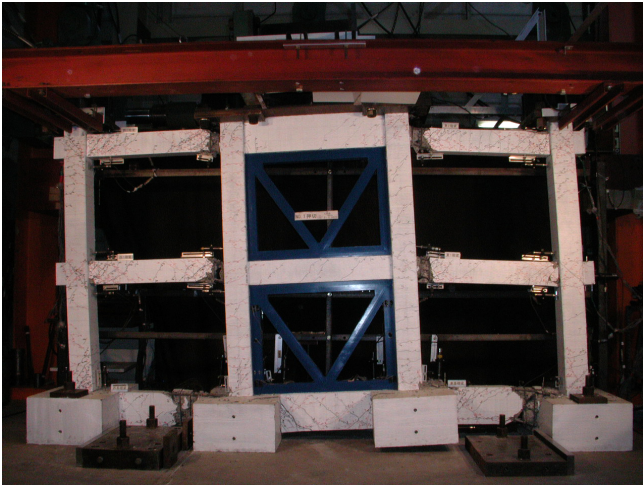


(a) Specimen No.1

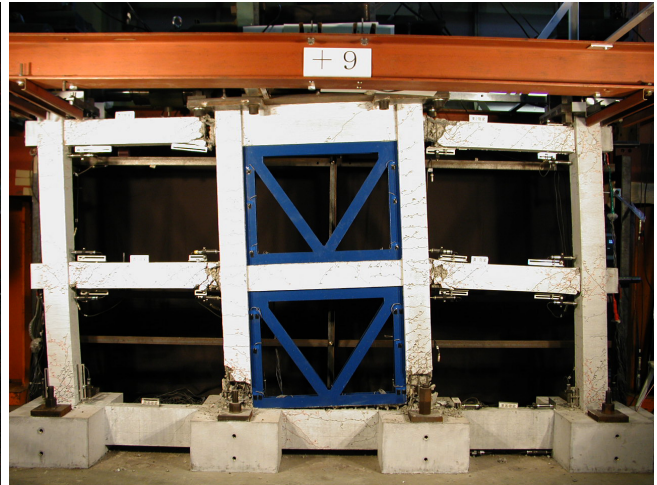


(b) Specimen No.2

**Fig. 4 Crack patterns at end of test**

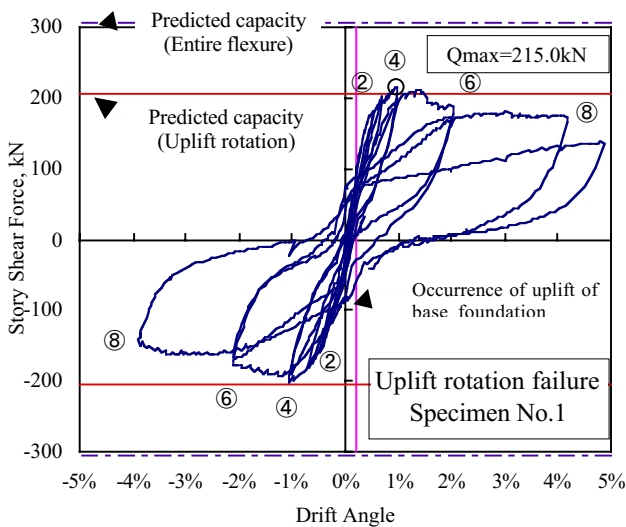


(a) Specimen No.1

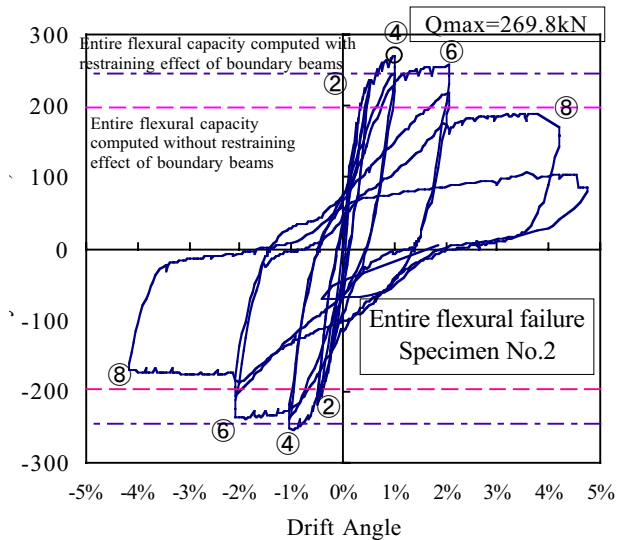


(b) Specimen No.2

**Photo. 1 Failure of specimens**



(a) Specimen No.1



(b) Specimen No.2

**Fig. 5 Story shear force- drift angle relations**

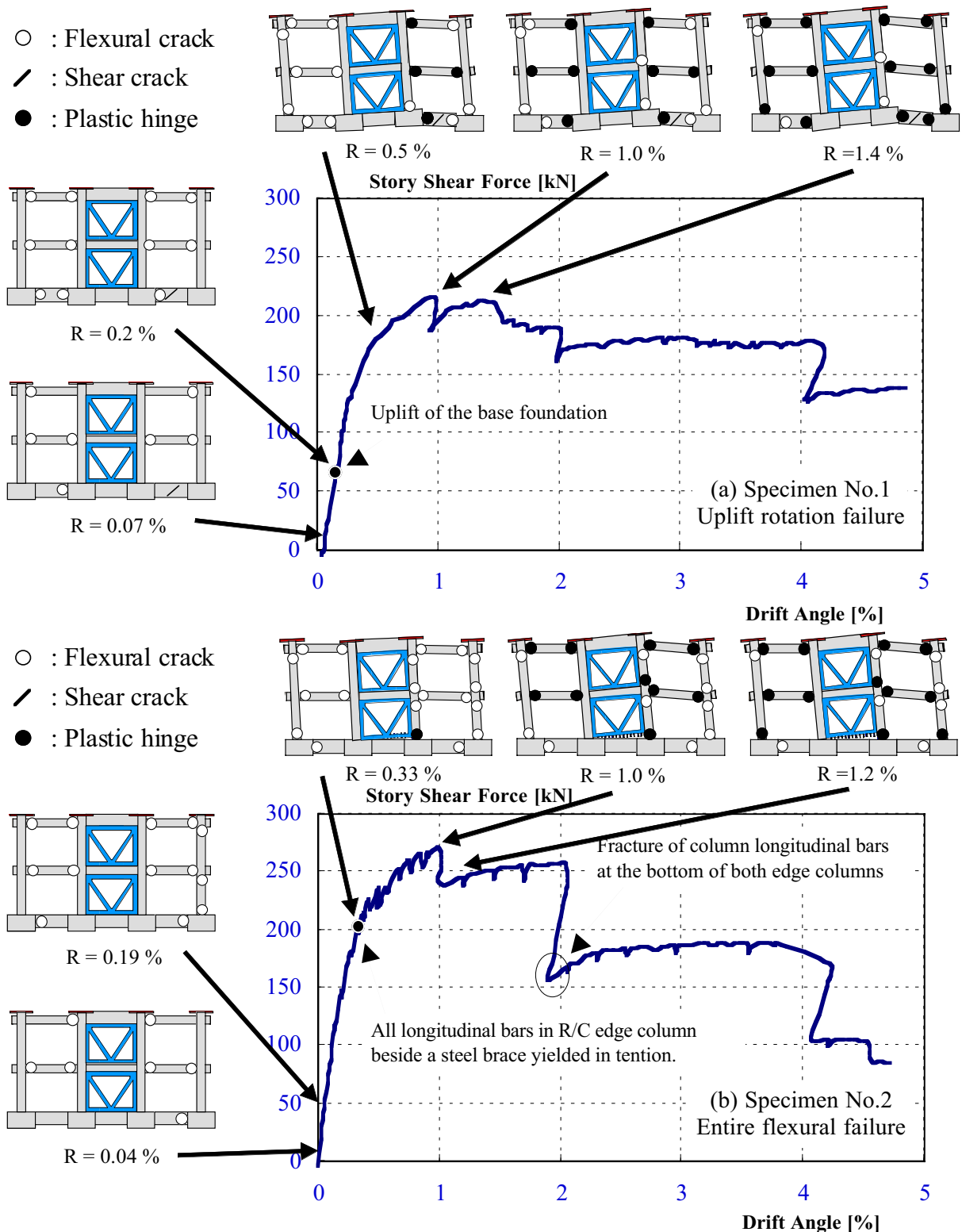


**Fig. 6 Envelope curves of story shear force - drift angle relation**

(a) Specimen No.1

Uplift of the base foundation under a multi-story steel brace occurred at the drift angle of 0.2 %. Collapse mechanism was formed at the drift angle of 1.4 %, developing flexural yielding at the end of boundary beams and the bottom of first story bare columns. Lateral resistance capacity decayed gradually due to concrete compressive failure at these hinge

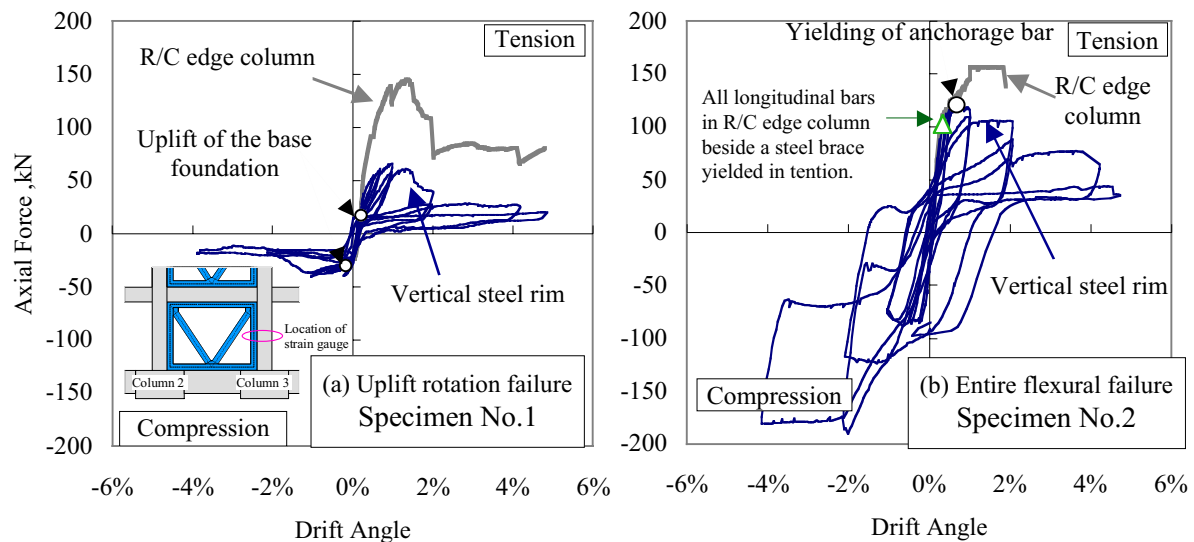


**Fig. 7 Axial force acting on vertical steel rim and R/C edge column**

regions after attaining the peak strength of 215.0 kN at the drift angle of 1 %. Obvious stiffness degradation caused by both base uplift and concrete crushing at hinge regions was observed after sixth loading cycle at the drift angle of 2 % as shown in **Fig. 5 (a)**.

Hysteresis loops showed a little pinching shape comparing with those for Specimen No.2.

#### (b) Specimen No.2

All longitudinal bars in R/C edge column beside a steel brace yielded in tension at the drift angle of 0.3 %. Lateral force resistance reached the maximum capacity of 269.8 kN at the drift angle of 1 %, forming plastic hinges at all boundary beam ends and cracking horizontally at the gap between horizontal steel rim and R/C foundation beam due to pull-out of anchorage bars.

Hereafter lateral resistance diminished abruptly by the concrete crushing and the fracture of column longitudinal bars at the bottom of both edge columns at the drift angle of 2 % in eighth loading cycle. Hysteresis loops showed a stable spindle shape until the drift angle of 2 %.

### 3.2 AXIAL FORCE ACTING ON VERTICAL STEEL RIM AND R/C EDGE COLUMN

Axial force acting on vertical steel rim of the brace, which was computed from measured strain at the mid-height in a first story brace, is shown in **Fig. 7**. Vertical steel rims did not yield for both specimens. Tensile axial force induced in R/C edge column beside a brace which was computed by measured strain of longitudinal bars at the mid-height of a first-story edge column is also shown in **Fig. 7**. In Specimen No.2, failed in entire flexure at the bottom of a multi-story steel brace, tensile axial force of vertical steel rim increased even after all longitudinal bars yielded at the bottom of R/C edge column, and attained the peak force with the yielding of anchorage bars at the bottom of the brace. The peak tensile force



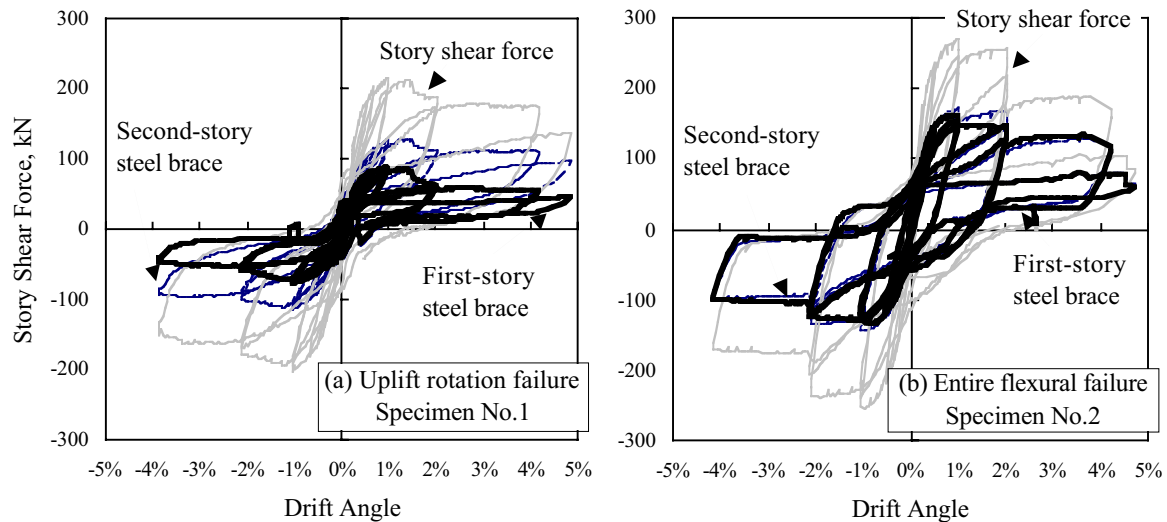


**Fig. 8 Horizontal shear force resisted by steel brace**

of vertical steel rim was three-quarters times that of axial force in R/C edge column at the drift angle of 1 %. Therefore it is important to take account of the contribution of vertical steel rim to entire flexural resistance at the bottom of a multi-story steel brace in addition to the longitudinal column bars.

### 3.3 HORIZONTAL SHEAR FORCE RESISTED BY STEEL BRACE

Shear force resisted by a steel brace can be obtained as horizontal component of axial force in diagonal steel chords subjected to tension and compression, which was computed from measured strain at these chords, and is shown in **Fig. 8**. Thick or thin solid lines represent the lateral shear component of first- or second-story steel brace respectively. Lateral resistance of the first-story steel brace in Specimen No.1, failed by uplift rotation of a multi-story steel brace, was by 30 percent smaller than that of the second-story steel brace since lateral force applied at the top of a multi-story steel brace was carried to the ground through neighboring beams and columns escaping from a steel brace. On the contrary, lateral resistance of the first-story steel brace in Specimen No.2, failed in entire flexure at the bottom of a multi-story steel brace, was almost equal to that of the second-story steel brace. The ratio of shear force shared by a first-story steel brace to entire lateral resistance of the specimen was 38 % for Specimen No.1 and 60 % for Specimen No.2.

### 3.4 TENSILE STRESS OF ANCHORAGE BAR

Tensile stress of anchorage bars connecting the bottom of steel rim of a multi-story steel brace with a foundation beam for Specimen No.2 is shown in **Fig. 9**. Tensile stress of the closest anchorage bar to a R/C edge column reached the yield stress and decreased after the

**Table 2 Measured and computed lateral strength of specimens**

Specimen	Measured Strength (kN)	Computed Strength (kN)				Ratio of computed to measured strength	
		Yielding of diagonal chord in brace	Type 3[*] failure	Type 3[**] failure	Brace base rotation failure		
No.1	215.0	490.1	256.9	305.1	205.1	0.95	
No.2	269.8	468.3	198.0	246.2	—	[*] 0.73	[**] 0.91

[\*], [\*\*]: Computed lateral strength of Type 3 failure without or with consideration of restraining effect by boundary beams respectively

drift angle of 0.76 % due to pull-out of the bar caused by the entire flexural resistance. Tensile stress of second and third anchorage bars denoted as A2 and A3 reached peak stress prior to yielding because horizontal crack occurred in the foundation beam, crossing these anchorage bars and pull-out force was reduced.

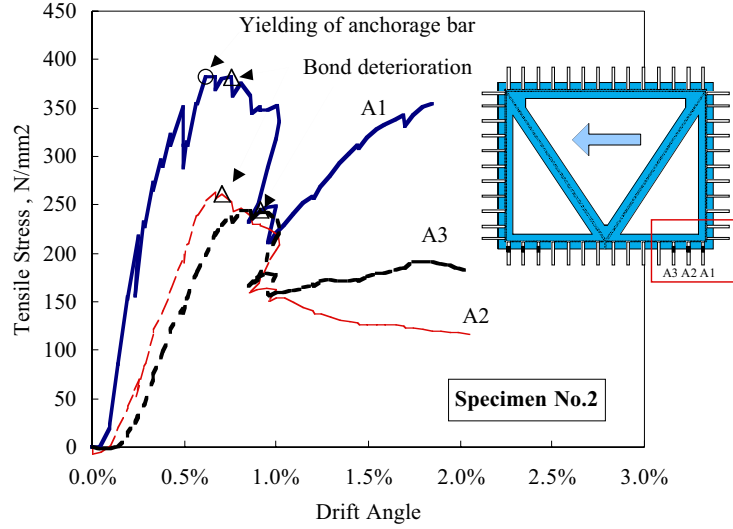


**Fig. 9 Tensile stress of anchorage bars**

#### 4. DISCUSSIONS

##### 4.1 LATERAL STRENGTH

Lateral strength  $Q_{max}$  obtained by the test is compared with the computed strength  $Q_{cal}$  by Eq.(1) and listed in **Table 2**.

$$Q_{cal} = Q_{c1} + Q_{c4} + Q_{Bf} \quad (1)$$

where  $Q_{c1}$  and  $Q_{c4}$ : lateral strength of a R/C isolated column (i.e., Column 1 and Column 4 in **Fig. 10**) computed by Eq.(2) since shear strength was greater than flexural strength for both columns.

$$Q_{c1}, Q_{c4} = \frac{2M_{cu}}{h} \quad (2)$$

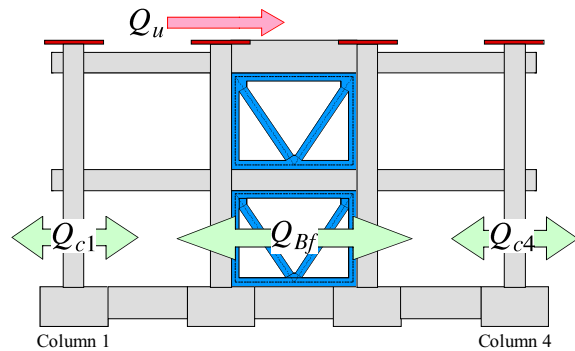


**Fig. 10 Lateral resistance of frame**

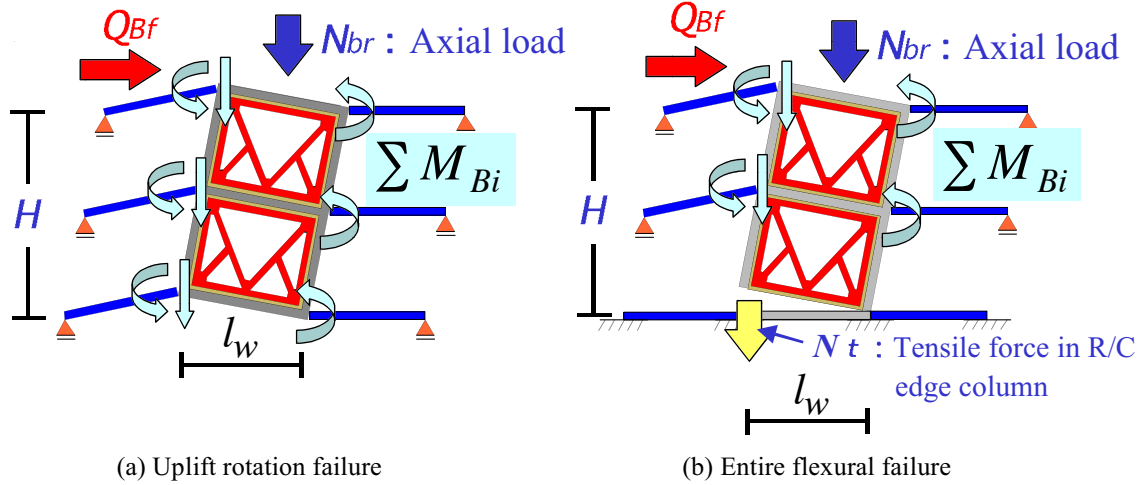


**Fig. 11 Lateral shear resistance of R/C unit frame with multi-story steel brace**

where  $h$  : clear height of the column and  $M_{cu}$  : ultimate bending moment at column critical section which can be computed by Eq.(3).

$$M_{cu} = 0.8a_t \cdot \sigma_y \cdot D + 0.5N_{col} \cdot D \left( 1 - \frac{N_{col}}{bD \cdot \sigma_B} \right) \quad (3)$$

where  $a_t$  ,  $\sigma_y$  : sectional area and yield strength of tensile longitudinal reinforcement in the column,  $D$  : column depth,  $N_{col}$  : column axial load,  $b$  : column width and  $\sigma_B$  : concrete compressive strength.

$Q_{Bf}$  : lateral shear resistance shared by the R/C central bay containing a multi-story steel brace which can be computed by Eq.(4) as illustrated in **Fig. 11**.

For uplift rotation failure,

$$Q_{Bf} = \frac{0.5N_{br} \cdot l_w + \sum_i M_{Bi}}{H} \quad (4.a)$$

For entire flexural failure (i.e., Type 3),

$$Q_{Bf} = \frac{a_t \cdot \sigma_y \cdot l_w + 0.5N_{br} \cdot l_w + \sum_i M_{Bi}}{H} \quad (4.b)$$

where  $a_t$  ,  $\sigma_y$  : sectional area and yield strength of tensile longitudinal reinforcement of edge column beside a steel brace,  $N_{br}$  : compressive axial load imposed at the center of a steel brace,  $l_w$  : center-to-center distance between R/C edge columns beside a steel brace,  $\sum_i M_{Bi}$  : sum of the flexural yielding moment of boundary beams framing into a multi-story steel brace, including the restraining moment due to shear force of boundary beams framing into uplift edge column, and  $H$  : height between the center of a foundation beam and a top floor beam (1665 mm). It is assumed for Eq.(4) that concentrated roof-level load was applied to the R/C central bay containing a multi-story steel brace.

Lateral strength measured in Specimen No.1 agreed well with that computed by taking account of restraining effect of both boundary and foundation beams on uplift rotation.

For Specimen No.2, predicted lateral strength of 198.0 kN without consideration of restraining effect by boundary beams, i.e., lateral shear strength obtained by extracting the term of  $\sum_i M_{Bi}$  from Eq.(4.b), was almost equal to measured resistance when all longitudinal bars yielded in a tensile edge column. In the test lateral resistance increased and attained the peak strength with the formation of beam hinge mechanism. Therefore lateral strength for entire flexural failure at the bottom of a multi-story steel brace was computed by Eq.(4.b) and it was 91 percent of measured lateral strength. It seems that contribution of the vertical steel rim to entire flexural resistance at the bottom of a brace may be considered to the extent that anchorage of a steel brace to R/C foundation beam is effective to carry tensile axial force in vertical steel rim to the foundation.

#### 4.2 CONTRIBUTION TO LATERAL RESISTANCE

Contribution of a multi-story steel brace and isolated R/C columns to lateral resistance of specimens is shown in **Fig. 12**. Shear force resisted by the R/C central bay containing a multi-story steel brace,  $Q_{Bf}$ , was computed by the same manner as Eq.(4) using measured strains of longitudinal bars in boundary beams and edge columns for each peak in loading cycles. For Specimen No.2, pull-out resultant force of three anchorage bars at the bottom of a multi-story brace was regarded as effective on entire flexural resistance cooperating with tensile force in a R/C edge column, and was added to right-hand side of Eq.(4.b). Shear resistance of isolated R/C columns,  $Q_{c1} + Q_{c4}$ , was calculated as follows ;

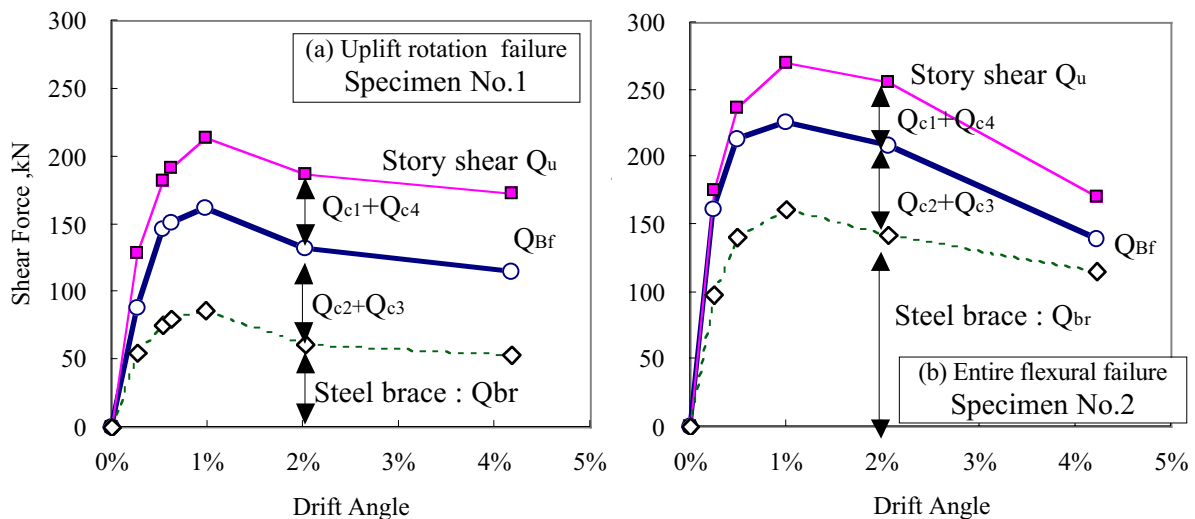


**Fig. 12 Contribution to lateral resistance**

$$Q_{c1} + Q_{c4} = Q_u - Q_{Bf} \quad (5)$$

where  $Q_u$  : measured story shear force. Lateral shear force,  $Q_{Br}$ , shared by diagonal steel chords in the first-story brace, obtained in Chapter 3.3, is also shown in **Fig. 12**.

Shear force resisted by isolated R/C columns,  $Q_{c1} + Q_{c4}$ , was almost same for both specimens at the drift angle of 2 %, developing flexural yielding capacity of those columns. This means that the computation method for shear force resisted by a central bay,  $Q_{Bf}$ , is roughly adequate. The difference between  $Q_{Bf}$  and  $Q_{Br}$ , which is shown as  $Q_{c2} + Q_{c3}$  in **Fig. 12**, indicates shear force shared by two R/C edge columns beside a brace. For Specimen No.2, failed in entire flexure at the bottom of a brace,  $Q_{c2} + Q_{c3}$  was greater than  $Q_{c1} + Q_{c4}$  because lateral force was carried through punching shear in the edge column subjected to compression.

#### 4.3 DEFORMATION PERFORMANCE

Standard for evaluation of seismic capacity of existing R/C buildings [2] was revised in 2001 in Japan. Deformation ability for a multi-story steel brace which fails by uplift rotation of the base or entire flexural yielding at the bottom of a brace (i.e., Type 3 failure) can be estimated according to this standard. Deformation ability is expressed by the ductility index denoted as  $F$  which is a function of the ductility factor as follows ;

$$F = \frac{\sqrt{2R_{mu}/R_y - 1}}{0.75(1 + 0.05R_{mu}/R_y)} \quad (6)$$

where  $R_{mu}$  : ultimate story drift angle of R/C members and  $R_y$  : yielding story drift angle assumed to be 0.67 %.

The  $F$  index for a multi-story steel brace with boundary beams is computed by Eq.(7).

$$F = wq \cdot wF + \Sigma(bq \cdot bF) \quad (7)$$

where,  $wF$ ,  $bF$  : ductility index for an isolated steel brace and a R/C boundary beam respectively which can be estimated by Eqs.(8) and (9);

$$\text{for uplift rotation failure,} \quad wF = 3.0 \quad (8.a)$$

$$\text{for entire flexural failure (Type 3),} \quad wF = 2.0 \quad (8.b)$$

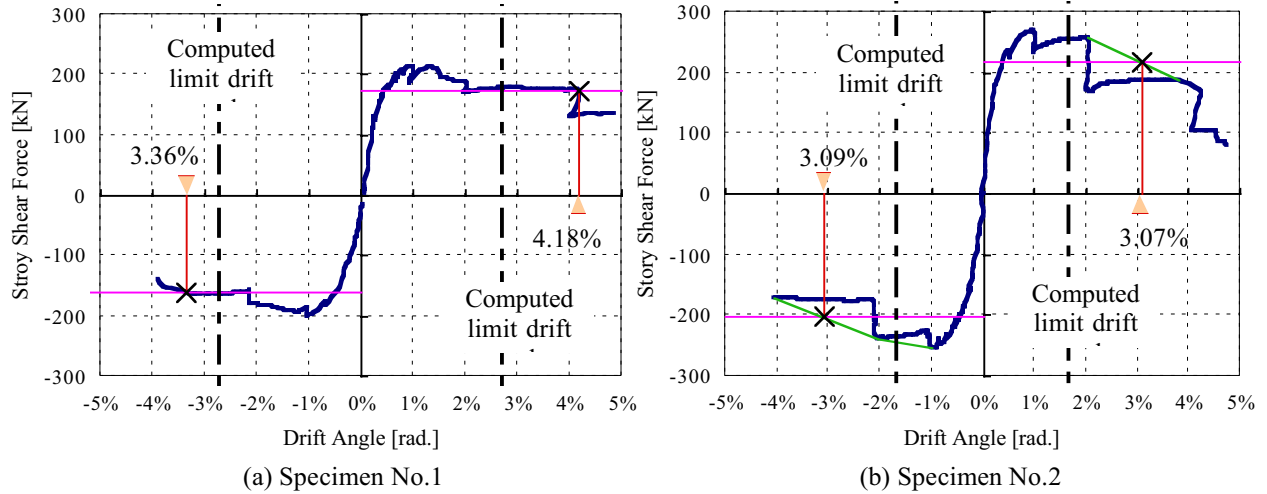


**Fig. 13 Ultimate limit drift angle obtained in test and computation**

$$\text{if } bQ_{su} / bQ_{mu} \leq 0.9, \quad bF = 1.27 \quad (9.a)$$

$$\text{if } bQ_{su} / bQ_{mu} \geq 1.3, \quad bF = 3.5 \quad (9.b)$$

if  $0.9 \leq bQ_{su} / bQ_{mu} \leq 1.3$ , the  $bF$  index shall be computed by the linear interpolation between Eq.(9.a) and Eq.(9.b), where  $bQ_{su}$ ,  $bQ_{mu}$  : ultimate shear and flexural strength of a boundary beam respectively.

$$wq = \frac{wM}{wM + \sum bM} \quad (10.a)$$

$$bq = \frac{bM}{wM + \sum bM} \quad (10.b)$$

where  $wM$  : brace contribution to ultimate resisting moment at the height where the lateral strength of a multi-story steel brace was decided and  $bM$  : ultimate resisting moment of a boundary beam framing into a multi-story steel brace.

The  $F$  index taken as explained above was 2.96 for Specimen No.1 and 2.38 for Specimen No.2 as listed in **Table 3**. These values correspond to the drift angle of 2.70 % and 1.68 % respectively, which were converted through Eq.(6).

On the other hand, ultimate limit drift angle was obtained in the test as shown in **Fig. 13** which is defined as the drift angle when the lateral resistance descended to 80 % of peak strength for the envelope curve of the story shear force - drift angle relation. Average ultimate limit drift angle for positive and negative loading directions was 3.8 % for

**Table 3 Ductility index and ultimate limit drift angle**

	R : Limit Drift Angle	Specimen No.1		Specimen No.2	
		Positive Loading	Negative Loading	Positive Loading	Negative Loading
Test Result	R	4.18%	3.36%	3.07%	3.09%
	R(average)	3.77%		3.08%	
Computed Result	$F$ index	2.96		2.38	
	R	2.70%		1.68%	

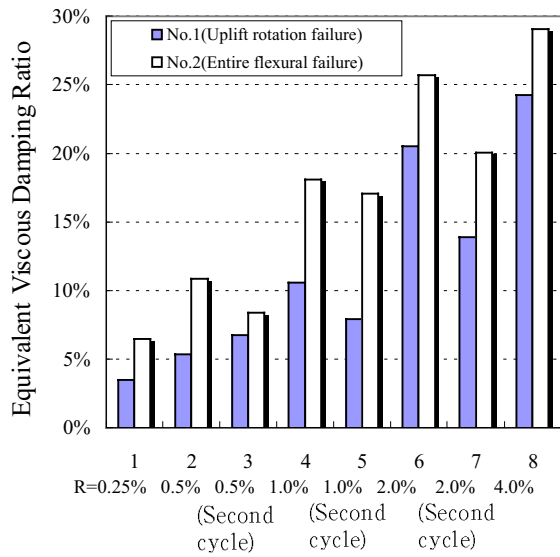


**Fig. 14 Equivalent viscous damping ratio**

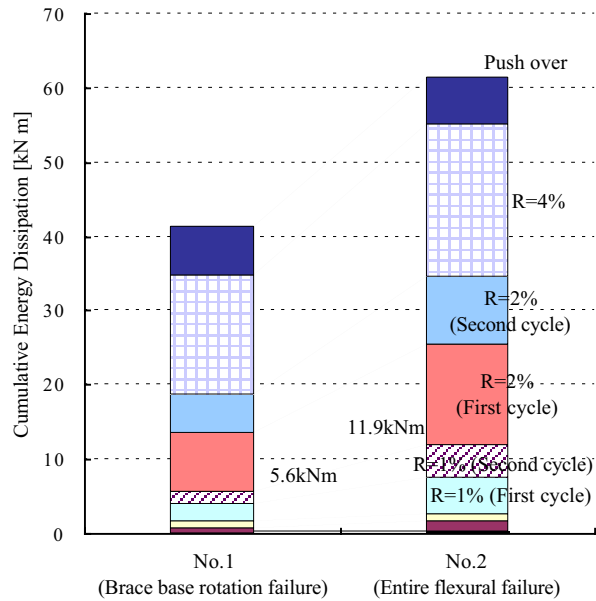


**Fig. 15 Cumulative energy dissipation**

Specimen No.1 and 3.1 % for Specimen No.2. This indicates that ductility performance in the case of uplift rotation failure of a multi-story steel brace was superior to that for entire flexural failure due to tensile yielding of all longitudinal bars in a R/C edge column as predicted by the  $F$  indices. Computed ultimate limit deformations based on the  $F$  index for both specimens were conservative comparing with test results. Ultimate limit drift angle for Specimen No.2 can be supposed to be 2 % approximately if the effect of cyclic load reversals on seismic resistant performance is taken into account, because significant lateral resistance degradation occurred after the drift angle of 2 %. Then predicted ultimate limit drift angle of 1.68 % for Specimen No.2 seems to be adequate.

#### 4.4 ENERGY DISSIPATION

The equivalent viscous damping ratio for each loading cycle in story shear force - drift angle relations is shown in **Fig. 14**. The equivalent viscous damping ratio was calculated by normalizing the dissipated energy within half a cycle by the strain energy at peak of an equivalent linearly elastic system. The equivalent viscous damping ratio in Specimen No.1 was smaller than 10 % at the drift angle less than or equal to 1 % and increased rapidly to 20 % at sixth loading cycle with the formation of beam hinge mechanism. The equivalent viscous damping ratio in Specimen No.2 exceeded 10 % even at second loading cycle corresponding to the drift angle of 0.5 % since all longitudinal bars yielded in the R/C edge column beside a steel brace. The equivalent viscous damping ratio in Specimen No.2 was greater than that in Specimen No.1 for all loading cycles. Therefore it is pointed out that the entire flexural failure at the bottom of a multi-story steel brace absorbed more hysteresis energy than the uplift rotation failure.

Cumulative energy dissipation is shown in **Fig. 15**. The amount of cumulative energy dissipation for Specimen No.2 was by 113 percent greater than that for Specimen No.1 at the drift angle of 1 % at which the peak lateral strength was achieved, and by 50 percent greater than that for Specimen No.1 at the last loading stage.

## 5. CONCLUSIONS

Earthquake resistant performance in plane R/C frames strengthened by a multi-story steel brace was investigated through the tests under cyclic load reversals focusing on the base uplift rotation of the brace and the entire flexural failure at the bottom of the brace caused by tensile yielding of all longitudinal bars in a R/C edge column. The following concluding remarks can be drawn from the present study:

(1) Lateral resistance for the base uplift rotation of a multi-story steel brace decreased gradually after flexural yielding occurred at the end of boundary beams and the bottom of first-story isolated columns at the drift angle of 1.4 %. Lateral strength computed by taking account of restraining effect of both boundary and foundation beams on uplift rotation agreed well with the test result.

(2) For the specimen failed in entire flexure at the bottom of a multi-story steel brace, all longitudinal bars in a R/C edge column subjected to tension beside the brace yielded at the drift angle of 0.3 %. Hysteresis loops showed a spindle shape until the drift angle of 2 %, stably dissipating hysteresis energy. However lateral resistance diminished abruptly by concrete crushing and fracture of column longitudinal bars at the bottom of both edge columns. Lateral strength computed by considering both flexural resistance attributed to tensile force in a R/C edge column and resisting moment of boundary beams same as the case of the base uplift rotation underestimated a little that obtained in the test. Contribution of the vertical steel rim to the entire flexural resistance should be taken into account if anchorage of the bottom of a multi-story steel brace to R/C foundation beam is sufficient to carry tensile axial force in vertical steel rim to the foundation.

(3) Ultimate limit deformations in two specimens estimated by considering respective deformation ability of boundary beams and an isolated multi-story steel brace were conservative comparing with test results.



(4) Ductility performance in the brace uplift rotation failure was superior to that in the entire flexural failure due to tensile yielding of all longitudinal bars in a R/C edge column.

(5) The amount of energy dissipation in the entire flexural failure at the bottom of a multi-story steel brace was by 50 percent greater than that in the brace uplift rotation failure.

(6) It is judged that earthquake resistant performance of strengthened R/C frames which is controlled by the entire flexural failure at the bottom of a multi-story steel brace is superior to that in the brace uplift rotation failure within the range of the drift angle of 2 %.

### **ACKNOWLEDGMENT**

The study reported in the paper was sponsored by a Grant-in-aid for Scientific Research of Japan Society for the Promotion of Science (Head researcher : K. Kitayama). The test was executed by Mr. H. Kato, Rui Design Room Co.Ltd, as a part of the master thesis in Tokyo Metropolitan University.

### **REFERENCES**

- [1] Kato, D., H. Katsumata and H. Aoyama : Effect of Wall Base Rotation on Behavior of Reinforced Concrete Frame-Wall Buildings, Proceedings of the Eighth World Conference on Earthquake Engineering, San-Francisco, July, 1984.
- [2] Japan Building Disaster Prevention Association : Standard for Evaluation of Seismic Capacity of Existing Reinforced Concrete Buildings, revised in 2001, (in Japanese).